Available online at www.sciencedirect.com
ScienceDirect
Carbohydrate Research 342 (2007) 2494–2499
Carbohydrate RESEARCH

Note

Mass synthesis of single-crystal gold nanosheets based on chitosan

Dongwei Wei, Weiping Qian,* Yi Shi, Shaohua Ding and Yan Xia

State Key Laboratory of Bioelectronics, School of Biological Science and Medical Engineering, Southeast University, Nanjing 210096, PR China

Received 3 April 2007; received in revised form 25 June 2007; accepted 3 July 2007
Available online 13 July 2007

Abstract—Single-crystal Au nanosheets with {1 1 1} planes as basal surfaces have been synthesized on the basis of the polysaccharide chitosan. The preferential adsorption of polar groups in chitosan molecules on {1 1 1} planes of Au nuclei may account for the formation of anisotropic nanosheets. Appropriate precursor ($HAuCl_4$) concentrations are vital for the formation of Au nanosheets. The Au nanostructures thus prepared exhibit interesting shape-dependent optical properties. This convenient, environmentally friendly and low-cost route may be amenable to mass production.

Keywords: Au nanosheets; Chitosan; Precursor concentrations

Metal nanoparticles have attracted intensive research interest because of their important applications in catalysis, sensing, and surface-enhanced Raman scattering (SERS).[1–7] As a result, many methods have been developed for synthesis of metal nanoparticles in a wide range of nonspherical shapes, including wires/rods, rings, cubes, sheets, tetrahedral bipyramids, hollow nanostructures, and branched nanocrystals.[8–14] Among these anisotropic nanostructures, two-dimensional (2D) Au nanosheets attract much attention for their unique optical features and potential applications in gas sensors, in the fabrication of nanodevices and substrate materials, and also for inducing hyperthermia in tumors.[15–18] Although there have been several updates on the synthesis of Au nanosheets,[8,15–19] the mass fabrication of such 2D nanomaterials by a facile, environmentally friendly and low-cost route remains a challenge.

Recent researches have largely been focused on the preparation of nanomaterials using biomolecules and bioorganisms. Exposure of the fungus Verticillium to aqueous $AuCl_4^-$ or Ag^+ ions resulted in the intracellular reduction of metal ions and the formation of gold and silver nanoparticles.[20,21] Noble metal (Ag, Au, Pt, Pd) nanoparticles have been synthesized in porous cellulose fibers that act as nanoreactors.[22] Sastry and co-workers also reported a new biological method for preparing triangular gold nanoprisms with lemon grass extract.[9] Carbohydrates, like sucrose,[23] β-D-glucose,[24] and starch[24,25] have been introduced as reducing and/or stabilizing agents for the preparation of metal nanoparticles. Chitosan is a β-(1→4)-linked D-glucosamine derivative of the polysaccharide chitin, a cellulose-like biopolymer widely distributed in nature. The chemical structures of chitin and chitosan are shown in Figure 1. Due to its unique polycationic, chelating, and film-forming properties, chitosan has been widely used in cosmetics, pharmaceuticals, food science, wastewater treatment, biotechnology and in other areas.[26] Chitosan has been adopted by Esumi et al. as a stabilizing agent in the preparation of gold nanoparticles.[27] It has been recently reported that chitosan is more than a stabilizing agent and that $AuCl_4^-$ ions can be reduced to zerovalent gold nanoparticles by chitosan itself without any additional reducing agent.[28,29] In this work, we demonstrate the feasibility of preparing single-crystal Au nanosheets on the basis of the polysaccharide chitosan. To the best of our knowledge, there are no reports on the mass synthesis of such large 2D Au nanosheets based on this technique.

* Corresponding author. Tel./fax: +86 25 83795719; e-mail: wqian@seu.edu.cn

0008-6215/$ - see front matter © 2007 Published by Elsevier Ltd.
doi:10.1016/j.carres.2007.07.001

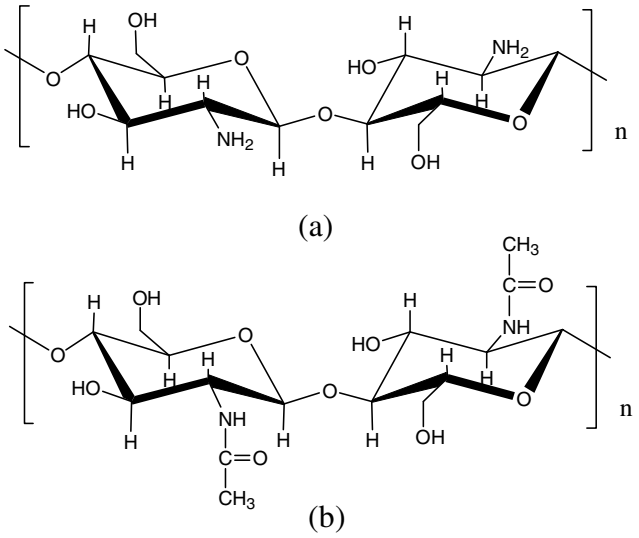

Figure 1. Structures of (a) chitosan and (b) chitin.

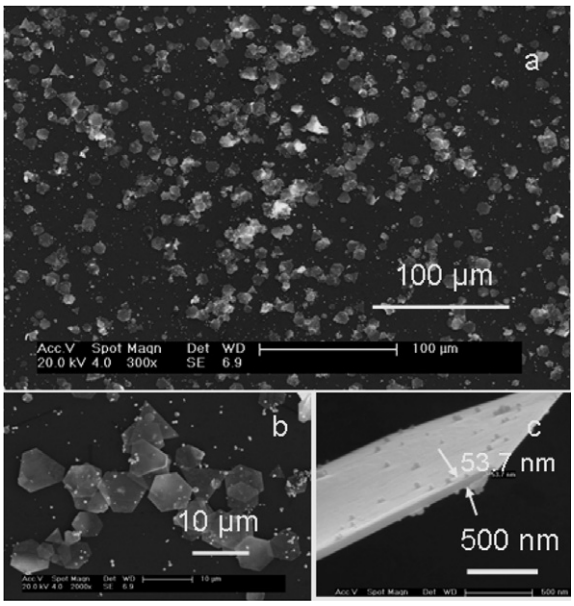

Figure 2. FESEM images of the sample synthesized by reduction of a 20 mM $HAuCl_4$ solution with chitosan at 100 °C. (a) Low magnification. (b) Enlarged images from products in (a). (c) The thickness of a single nanosheet.

In a typical synthesis, 5 mL of 4–20 mM $HAuCl_4$ was added to 6 mL of 3.46 mg/mL chitosan solution under stirring at room temperature. After 15 min, the mixture was transferred to a 12.5×2 cm cuvette and kept in a water bath at 40–100 °C for about 6 h. There was no obvious change in color at the beginning. After several minutes, the mixtures changed from a light yellow solution ($AuCl_4^-$) to a golden solution containing glistening products that increased progressively with the reaction time. The resulting products were rinsed with deionized water and centrifuged (500*g*) to remove the residual reactants and possible contamination.

Figure 2 shows the field-emission scanning electron microscopy (FESEM) images of the products as prepared. The lower magnification image (Fig. 2a) indicates that the products are mainly composed of nanosheets with regular shape, together with a few nearly spherical particles. Most nanosheets are triangular or hexagonal, approximately a few microns across (Fig. 2b) and several tens of nanometers thick (Fig. 2c), as determined using FESEM.

The energy-dispersive spectrum (EDS) in Figure 3a confirms that the nanosheets obtained consist of only gold. Figure 3b shows the X-ray powder diffraction (XRD) pattern of the Au nanosheets. A very strong diffraction at 2θ 38.2° assigned to the {1 1 1} lattice plane of face-centered-cubic {fcc} Au crystal is detected, together with very weak diffraction from other planar planes of the nanosheets or a small amount of other Au nanostructures.[8,17] This result implies that the basal plane should be the {1 1 1} plane, which has planar geometry. Figure 3c presents the selected-area electron diffraction (SAED) pattern from one of the Au nanosheets. The SAED pattern viewed along a {1 1 1} direction is of hexagonal symmetry, indicating the single-crystal structure of the nanosheet. The spots could be indexed based on the fcc structured Au.[9] The presence of the fcc forbidden 1/3{4 2 2} reflections reveals that the surfaces of the nanosheets are atomically flat.[17] The reason for this may be either the existence of stacking faults lying parallel to the {1 1 1} surfaces and extending across the entire nanosheets, or a hexagonal-like monolayer on the nanosheet faces.[30]

The formation of Au nanosheets was found to be dependent on the precursor ($HAuCl_4$) concentrations. It is clear that when the $HAuCl_4$ concentration is 8 or 12 mM, the products are dominated by micro-sized Au nanosheets with regular shape (Fig. 4a and b). On decreasing the $HAuCl_4$ concentration, a large number of Au particles about 50 nm in size, together with a few nanosheets, are produced (Fig. 4c). This indicates that appropriate precursor concentration is vital for the generation of Au nanosheets.

It is well known that the optical properties of metal nanostructures are strongly related to their shape and size. The UV–vis–NIR absorption spectra of the gold nanostructures synthesized by the reduction of different concentrations of $HAuCl_4$ solution exhibit such shape-dependent features as shown in Figure 5. The optical absorption spectrum of the Au nanosheets prepared shows an obvious increase in the band about 500 nm and expanded steadily into to 1200 nm (curves a and b), in agreement with the results for Au nanosheets reported previously,[8,30,31] but in contrast to the optical absorption of Au nanoparticles at about 560 nm (curve c). This broad and asymmetric band may be arising from the higher order resonances of Au nanostruc-

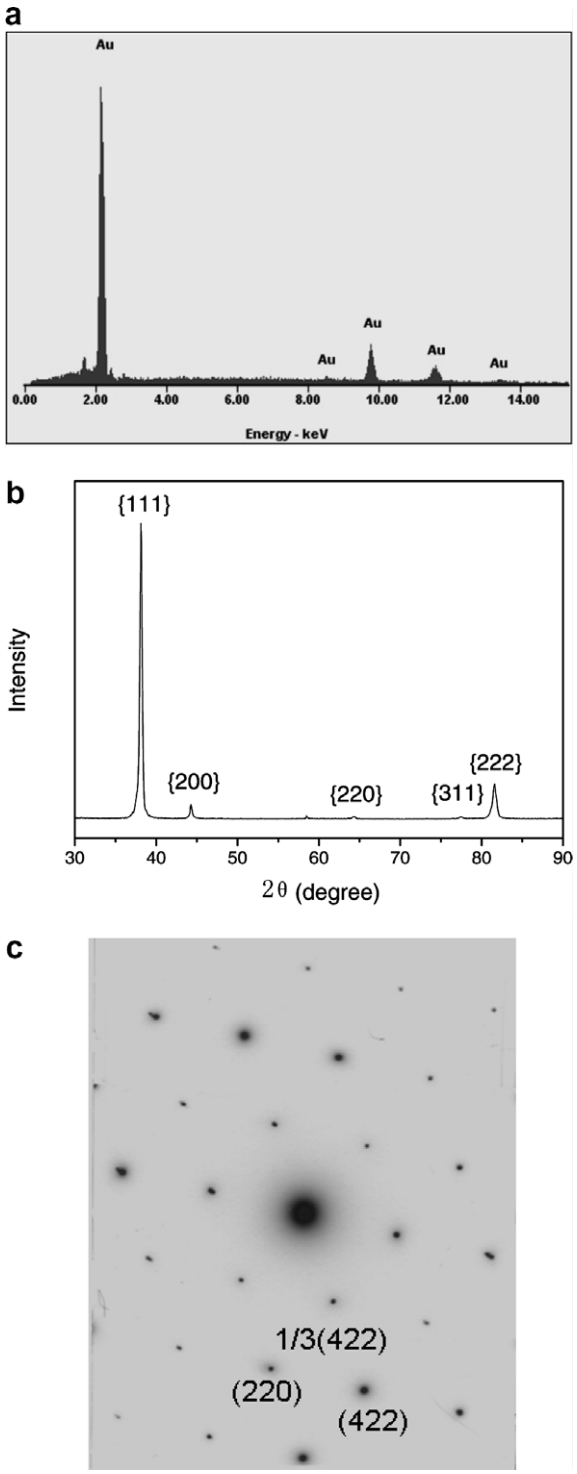

Figure 3. EDS (a) and XRD pattern (b) of the Au nanosheets. (c) SAED pattern of a single Au nanosheet.

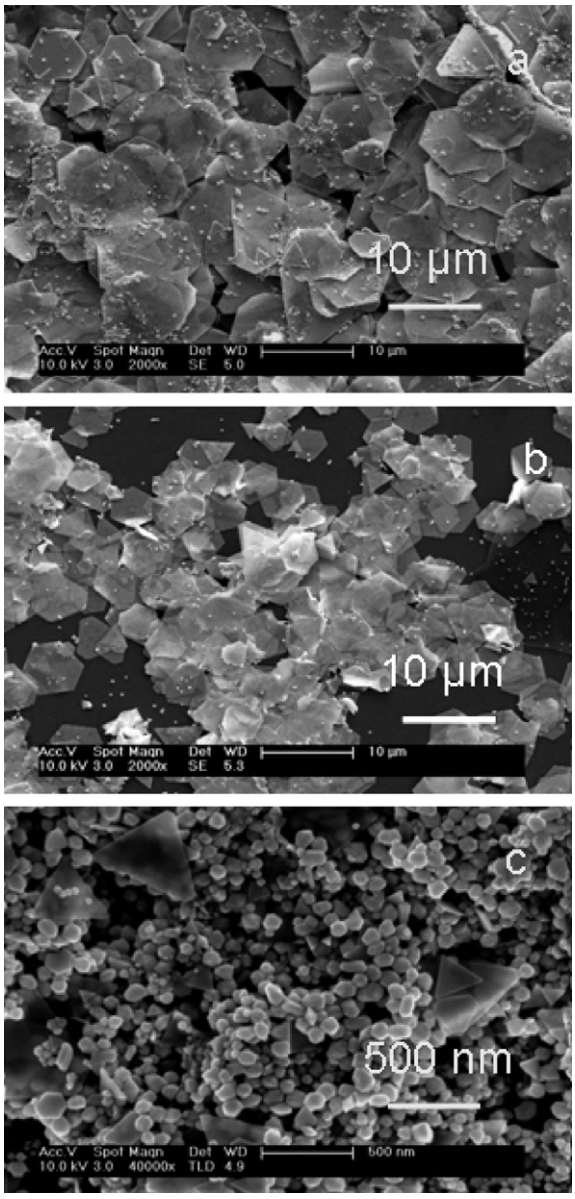

Figure 4. FESEM images of the sample synthesized by reduction of (a) 10 mM, (b) 6 mM, and (c) 4 mM $HAuCl_4$ solutions with chitosan at 60 °C.

tures.[8,31] Such an absorption extension of these Au nanosheets in the NIR region may be useful in biomedical applications.[17,32,33]

Figure 6 shows typical TEM images of six individual Au nanosheets with hexagonal, triangular-truncated or triangular shapes. A typical feature observed in Au nanosheet images is the appearance of a fascinating pattern, which is composed of fringes with different contrasts. The fringes resulting from bending contours have been consistently observed in TEM images of several types of nanocrystals and nanowires.[34] Although this remains to be proved, the origin of the bending may be due to the deviations from the planar geometry (for some reasons, for example, stacking faults).[34,35]

At present, the exact growth mechanism of the micro-sized Au nanosheets is not fully understood, although some explanations for the growth of anisotropic nanostructures have been presented by some groups.[36–38] The accepted opinion for the formation of nanosheets

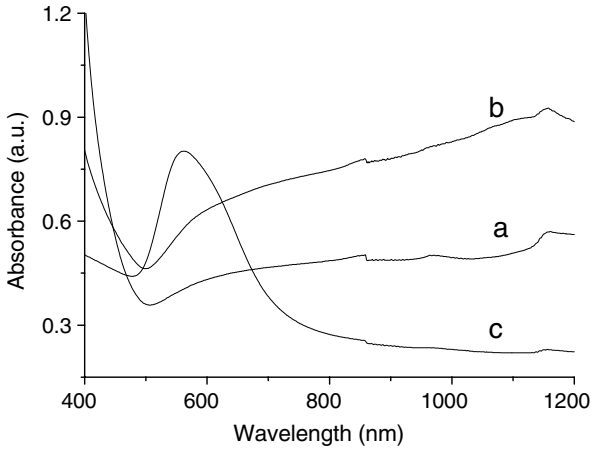

Figure 5. The UV–vis–NIR absorption spectra of a sample synthesized by reduction of (a) 10 mM, (b) 6 mM, and (c) 4 mM $HAuCl_4$ solution with chitosan at 60 °C.

usually involves the role of the preformed 'seed' and the appropriate capping reagents that are used to control the growth rate of various faces of the seeds. It is known that polymers are often used to prepare metal nanoparticles, in which the polar groups interact directly with the particle surface and strongly influence the shape of the particles.[8,19] Here we suggest that, though the exact role of chitosan is not clear, Au monomers are obtained by reducing $AuCl_4^-$ ions with chitosan molecules and/or some molecules induced by reaction.[17] When the concentration of gold atoms has reached supersaturation, a system that is far from the minimum free-energy configuration, they start to nucleate and grow.[37] Then at a favorite chitosan coverage, polar groups (such as hydroxyl and/or amino groups) in the chitosan molecules adsorb preferentially on the sites of the {1 1 1} planes of Au nuclei, which greatly decrease the surface energy of the {1 1 1} planes and lead to preferential growth along the ⟨1 1 0⟩ directions. Consequently, this favors the formation of anisotropic Au nanosheets with triangular, hexagonal, or truncated shapes. On the other hand, excessive chitosan coverage on the surfaces of gold seeds would induce a simultaneous growth for different crystal faces, resulting in an enhanced yield of nanoparticles. This suggests that the formation of large Au nanosheets needs specific conditions, such as an appropriate chitosan to $HAuCl_4$ ratio.

We have demonstrated a facile route for the mass synthesis of anisotropic Au nanosheets with a regular shape on the basis of chitosan. The resulting products were characterized by SEM, TEM, SAED, EDX, XRD, and UV–vis–NIR measurements. Investigation reveals that the Au nanosheets as prepared are single-crystal with the {1 1 1} plane as the basal surfaces. The generation of Au nanosheets was found to be dependent on the precursor ($HAuCl_4$) concentrations. The abundant source of raw materials and the ease of the synthesis make the approach a promising candidate for mass production.

1. Experimental

1.1. Synthesis

Chitosan flakes, from crab shells, (Practical grade >85% deacetylated; Brookfield viscosity >200.000 cps) were purchased from Aldrich Chemical Co. Hydrochloroau-

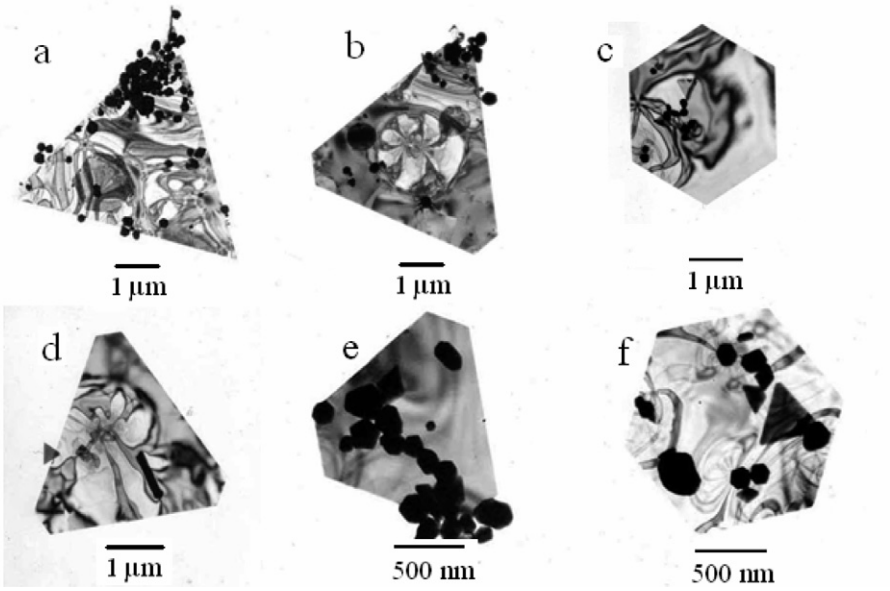

Figure 6. Representative TEM images of an individual Au nanosheet synthesized utilizing chitosan at different parameters: (a, b) 20.0 mM $HAuCl_4$, 100 °C; (c, d) 10.0 mM $HAuCl_4$, 40 °C; (e, f) 10.0 mM $HAuCl_4$, 80 °C.

ric acid and acetic acid were of analytical grade. Solutions were prepared with triply distilled water. All compounds were used as received. Chitosan was dissolved in 1% acetic acid solution. Due to the poor solubility of chitosan, the mixture was kept overnight until a clear solution was obtained. For the synthesis of Au nanosheets, 5 mL of 4–20 mM $HAuCl_4$ was added to 6 mL of a 3.46 mg/mL chitosan solution under stirring at room temperature. After 15 min, the mixture was transferred to a 12.5 $\times$ 2 cm cuvette and kept in a water bath at 40–100 °C until a golden solution was obtained (about 6 h). Before characterization, the resulting products were rinsed with deionized water and centrifuged (500*g*) to remove the residual reactants and possible contaminants.

1.2. Characterization

Scanning electron microscopy (SEM) images were recorded using a FEI SIRION field-emission scanning electron microscope equipped with an energy-dispersive spectrum (EDS). Transmission electron microscopy (TEM) was carried out on a JEM-2000EX microscope at an accelerating voltage of 120.0 kV. The samples were prepared by placing a drop of an aqueous dispersion of the Au products on a carbon-coated copper grid. The SAED pattern of the Au nanostructures was collected from the TEM system. The optical properties of the Au nanosheets as prepared were measured by a Shimadzu UV–vis–NIR spectrophotometer (UV-3150). The Au products were characterized as water dispersions and as thin coatings of the same batch on a glass substrate. X-ray powder diffraction pattern (XRD, D/Max-RA, Cu Kα, 40 kV, 30 mA) was taken from a sample prepared by dropping an aqueous dispersion of the products on a silicon substrate and allowing the solvent to evaporate spontaneously at ambient temperature.

Acknowledgments

This research is supported by the National Nature Science Foundation of China (Nos. 20475009, 60121101, and 90406024-4), the Foundation for the Author of National Excellent Doctoral Dissertation of PR China (No. 200252), and the Foundation for the Excellent Doctoral Dissertation of Southeast University.

References

1. Millstone, J. E.; Park, S.; Shuford, K. L.; Qin, L.; Schatz, G. C.; Mirkin, C. A. *J. Am. Chem. Soc.* **2005**, *127*, 5312–5313.
2. Xiong, Y.; McLellan, M. J.; Chen, J. Y. *J. Am. Chem. Soc.* **2005**, *127*, 17118–17127.
3. Wakayama, H.; Setoyama, N.; Fukushima, Y. *Adv. Mater.* **2003**, *15*, 742–745.
4. Tan, Y.; Qian, W. P.; Ding, S. H.; Wang, Y. *Chem. Mater.* **2006**, *18*, 3385–3389.
5. Riboh, J. C.; Haes, A. J.; McFarland, A. D.; Yonzon, C. R.; Van Duyne, R. P. *J. Phys. Chem. B* **2003**, *107*, 1772–1780.
6. Larsson, M.; Lu, J.; Lindgren, J. *J. Raman Spectrosc.* **2004**, *35*, 826–834.
7. Ding, S. H.; Qian, W. P.; Tan, Y.; Wang, Y. *Langmuir* **2006**, *22*, 7105–7108.
8. Kan, C. X.; Zhu, X. G.; Wang, G. H. *J. Phys. Chem. B* **2006**, *110*, 4651–4656.
9. Shankar, S. S.; Rai, A.; Ankamwar, B.; Singh, A.; Ahmad, A.; Sastry, M. *Nat. Mater.* **2004**, *3*, 482–488.
10. Murphy, C. J.; Sau, T. K.; Gole, A. M.; Orendorff, C. J.; Gao, J. X.; Gou, L. F.; Hunyadi, S. E.; Li, T. *J. Phys. Chem. B* **2005**, *109*, 13857–13870.
11. Sau, T. K.; Murphy, C. J. *J. Am. Chem. Soc.* **2004**, *126*, 8648–8649.
12. Chen, Y. B.; Chen, L.; Wu, L. M. *Inorg. Chem.* **2005**, *44*, 9817–9822.
13. Wiley, B. J.; Xiong, Y. J.; Li, Z. Y.; Yin, Y. D.; Xia, Y. N. *Nano Lett.* **2006**, *6*, 765–768.
14. Wiley, B.; Sun, Y. G.; Mayers, B.; Xia, Y. N. *Chem. Eur. J.* **2005**, *11*, 454–463.
15. Shankar, S. S.; Rai, A.; Ahmad, A.; Sastry, M. *Chem. Mater.* **2005**, *17*, 566–572.
16. Ankamwar, B.; Chaudhary, M.; Sastry, M. *Synth. React. Inorg., Met.-Org., Nano-Met. Chem.* **2005**, *35*, 19–26.
17. Li, C. C.; Cai, W. P.; Cao, B. Q.; Sun, F. Q.; Li, Y.; Kan, C. X.; Zhang, L. D. *Adv. Funct. Mater.* **2006**, *16*, 83–90.
18. Dahanayaka, D. H.; Wang, J. X.; Hossain, S.; Bumm, L. A. *J. Am. Chem. Soc.* **2006**, *128*, 6052–6053.
19. Sun, X. P.; Dong, S. J.; Wang, E. K. *Langmuir* **2005**, *21*, 4710–4712.
20. Mukherjee, P.; Ahmad, A.; Mandal, D.; Senapati, S.; Sainkar, S. R.; Khan, M. I.; Parishcha, R.; Ajaykumar, P. V.; Alam, M.; Kumar, R.; Sastry, M. *Nano Lett.* **2001**, *1*, 515–519.
21. Mukherjee, P.; Ahmad, A.; Mandal, D.; Senapati, S.; Sainkar, S. R.; Khan, M. I.; Ramani, R.; Parischa, R.; Ajayakumar, P. V.; Alam, M.; Sastry, M.; Kumar, R. *Angew. Chem., Int. Ed.* **2001**, *40*, 3585–3588.
22. He, J. H.; Kunitake, T.; Nakao, A. *Chem. Mater.* **2003**, *15*, 4401–4406.
23. Qi, Z.; Zhou, H.; Matsuda, N.; Honma, I.; Shimada, K.; Takatsu, A.; Kato, K. *J. Phys. Chem. B* **2004**, *108*, 7006–7011.
24. Raveendran, P.; Fu, J.; Wallen, S. L. *J. Am. Chem. Soc.* **2003**, *125*, 13940–13941.
25. Vigneshwaran, N.; Nachane, R. P.; Balasubramanya, R. H.; Varadarajan, P. V. *Carbohydr. Res.* **2006**, *341*, 2012–2018.
26. Yi, H.; Wu, L. Q.; Bentley, W. E.; Ghodssi, R.; Rubloff, G. W.; Culver, J. N.; Payne, G. F. *Biomacromolecules* **2005**, *6*, 2881–2894.
27. Esumi, K.; Takei, N.; Yoshimura, T. *Colloids Surf. B* **2003**, *32*, 117–123.
28. Huang, H. Z.; Yang, X. R. *Biomacromolecules* **2004**, *5*, 2340–2346.
29. Wang, B.; Chen, K.; Jiang, S.; Reincke, F.; Tong, W.; Wang, D.; Gao, C. Y. *Biomacromolecules* **2006**, *7*, 1203–1209.
30. Guo, Z. R.; Zhang, Y.; Duan Mu, Y.; Xu, L. N.; Xie, S. L.; Gu, N. *Colloids Surf. A* **2006**, *278*, 33–38.
31. Sun, X. P.; Dong, S. J.; Wang, E. K. *Angew. Chem., Int. Ed.* **2004**, *43*, 6360–6363.

32. Hirsch, L. R.; Stafford, R. J.; Bankson, J. A.; Sershen, S. R.; Rivera, B.; Price, R. E.; Hazle, J. D.; Halas, N. J.; West, J. L. *Proc. Natl. Acad. Sci. U.S.A.* **2003**, *100*, 13549–13554.
33. Sershen, S. R.; West, J. L. *J. Biomed. Mater. Res.* **2000**, *51*, 293–298.
34. Rodríguez-González, B.; Pastoriza-Santos, I.; Liz-Marzán, L. M. *J. Phys. Chem. B* **2006**, *110*, 11796–11799.
35. Ding, Y.; Wang, Z. L. *J. Phys. Chem. B* **2004**, *108*, 12280–12291.
36. Wiley, B.; Sun, Y. G.; Chen, J. Y.; Cang, H.; Li, Z. Y.; Li, X. D.; Xia, Y. N. *MRS Bull.* **2005**, *30*, 356–361.
37. Burda, C.; Chen, X. B.; Narayanan, R.; El-Sayed, M. A. *Chem. Rev.* **2005**, *105*, 1025–1102.
38. Lofton, C.; Sigmund, W. *Adv. Funct. Mater.* **2005**, *15*, 1197–1208.